PAPER • OPEN ACCESS

Passive and hybrid mode locking in multi-section terahertz quantum cascade lasers

New Journal of Physics
The open access journal at the forefront of physics

Deutsche Physikalische Gesellschaft DPG
IOP Institute of Physics

Published in partnership with: Deutsche Physikalische Gesellschaft and the Institute of Physics

OPEN ACCESS

RECEIVED
24 November 2017

REVISED
17 April 2018

ACCEPTED FOR PUBLICATION
30 April 2018

PUBLISHED
24 May 2018

PAPER

Passive and hybrid mode locking in multi-section terahertz quantum cascade lasers

P Tzenov[1], I Babushkin[2,3], R Arkhipov[4,5], M Arkhipov[4,5], N Rosanov[5,6,7], U Morgner[2] and C Jirauschek[1]

[1] Department of Electrical and Computer Engineering, Technical University of Munich (TUM), D-80333 Munich, Germany
[2] Institute of Quantum Optics, Leibniz University Hannover, D-30167 Hannover, Germany
[3] Max Born Institute, D-12489 Berlin, Germany
[4] St. Petersburg State University, 199034 St. Petersburg, Russia
[5] ITMO University, 197101 St. Petersburg, Russia
[6] Vavilov State Optical Institute, Kadetskaya Liniya V.O. 5/2, St. Petersburg 199053, Russia
[7] Ioffe Institute, Politekhnicheskaya str. 26, St. Petersburg 194021, Russia

E-mail: petar.tzenov@tum.de

Keywords: quantum cascade lasers, passive mode locking, hybrid mode locking

Abstract

It is believed that passive mode locking is virtually impossible in quantum cascade lasers (QCLs) because of too fast carrier relaxation time. Here, we revisit this possibility and theoretically show that stable mode locking and pulse durations in the few cycle regime at terahertz (THz) frequencies are possible in suitably engineered bound-to-continuum QCLs. We achieve this by utilizing a multi-section cavity geometry with alternating gain and absorber sections. The critical ingredients are the very strong coupling of the absorber to both field and environment as well as a fast absorber carrier recovery dynamics. Under these conditions, even if the gain relaxation time is several times faster than the cavity round trip time, generation of few-cycle pulses is feasible. We investigate three different approaches for ultrashort pulse generation via THz quantum cascade lasers, namely passive, hybrid and colliding pulse mode locking.

1. Introduction

Quantum cascade lasers are unipolar, electrically pumped semiconductor devices in which the optical transition occurs between bound electron states in the conduction band of a specially designed quantum well heterostructure [1]. Due to the intersubband nature of the radiative transition, quantum cascade lasers (QCLs) are highly tunable and allow for the generation of coherent radiation in the underdeveloped terahertz and mid-infrared (MIR) portions of the electromagnetic spectrum.

Since the first experimental realization of a QCL in 1994 [2], this technology has experienced remarkable advancement, with some of the most notable milestones being the realization of a room temperature MIR QCL emitting power at the Watt level [3], the demonstration of a THz QCL operating at the record high temperature of 200 K [4], as well as the successful generation of broadband coherent frequency combs by free running devices both in the MIR and THz spectral regions [5, 6].

Naturally, it is also of great scientific and practical interest to enable the formation of short, mode locked pulses of light with QCLs. This would be a major advancement for THz and MIR spectroscopy as it will open up the stage for ultrafast optical experiments, such as for example time-resolved THz spectroscopy [7], with compact, on-chip, direct sources. Additionally, since mode locked pulses are frequency combs in the Fourier domain, ultrashort pulse generation via QCLs will provide an alternative approach to obtain broadband frequency combs.

Unfortunately, experience shows that QCLs are notoriously difficult to mode lock [8]. Active mode locking was achieved in the MIR and THz regime in 2009 and 2011, respectively, via active modulation of the injection current [8, 9]. The shortest pulse width demonstrated so far in QCLs is 2.5 ps in the THz regime [10]. First attempts to obtain passive mode locking (PML) in QCLs [11] were later identified as dynamic instabilities [12].

Also, the above mentioned generation of frequency combs in free running QCLs, which is closely related since it also relies on phase coupling between the modes, did not result in ultrashort pulse emission in time-domain, but in more complex periodic waveforms [13]. It is believed that, due to the ultrafast processes that govern intersubband transitions, active mode locking of QCLs is feasible only close to lasing threshold, whereas PML, in the traditional sense, is virtually impossible [12]. This is because the intrinsically short carrier relaxation times, typically several times smaller than the cavity round trip time, obstruct the formation of short bursts of light since the trailing edges of any propagating pulse would be amplified by the fast recovering gain [14]. As pointed out in [15], this extremely fast intersubband dynamics with upper state lifetimes on the ps or even sub-ps time scale is in sharp contrast to the situation in bipolar semiconductor and in solid state lasers where the gain recovery time typically exceeds the round trip time by a large amount. Thus, the QCL dynamics deviates significantly from the classical case of PML where slow or fast saturable absorbers (FSAs) can be used since the gain saturates with the average optical power [16]. Importantly, in THz QCLs, longer gain recovery times can be achieved than in MIR QCLs, where the upper–lower laser level spacing exceeds the longitudinal optical phonon energy (e.g., 36 meV in GaAs), promoting upper laser level depopulation by phonon emission. As a consequence, also the gain bandwidth, which is to a considerable part determined by lifetime broadening of the lasing transition [17], tends to be larger in MIR QCLs, with typical values of around 5 THz [18] as compared to 1 THz in terahertz QCLs [17, 19]. Since the achievable pulse duration for PML scales inversely with the gain width, this would also mean that shorter pulses should be achievable for MIR lasers. In the THz, this limitation has been circumvented with a heterogeneous active region, where broadband gain is obtained by stacking heterostructures designed for different wavelengths [10]. Furthermore, it should be taken into account that typical central lasing frequencies of (experimentally demonstrated, actively mode locked) MIR [12] and THz [10] QCLs differ by an order of magnitude or more, so the relative gain bandwidth in THz QCLs tends to be larger than in MIR designs. Notably, the shortest pulse durations for mode locked QCL operation have been achieved in the THz range [10]. The peak gain, on the other hand, can be adjusted by the pump current. As mentioned above, active mode locking has been demonstrated in QCLs only close to lasing threshold, which is largely set by the waveguide loss, with typical values of around 10 cm^{-1} for both MIR and THz devices [10, 12].

We believe that there is no fully conclusive evidence to support the claims that PML is impossible in QCLs. Based on our above comparison of mode locking in THz and MIR QCLs, we will here focus on THz structures, especially due to the intrinsically longer gain recovery times. Despite the central role of the gain dynamics, it has not been extensively studied for THz QCLs. In fact, to the our best knowledge, to present date there have been only two publications experimentally investigating the gain recovery time in bound-to-continuum (BTC) THz devices, and none in resonant-phonon QCLs. Interestingly, these experimental results indicate sub-threshold lifetimes on the order of several tens of picoseconds [20, 21]. These measurement techniques are based on a pump-probe experimental method where a perturbing resonant pump pulse is injected into the gain medium followed by a temporally detuned probe pulse interacting with the saturated gain. In [20], the photocurrent induced by stimulated emission between the upper and the lower laser level was recorded as a function of the delay between both pulses, and a Gaussian fit was used to infer the speed of the recovery of population in the upper laser state. The measured lifetimes were ≈50 ps which, as we will show, are long enough to enable mode locking. In fact one might argue that BTC QCLs are among the most optimal devices for mode locking, since the energy exchange between the propagating pulse and the saturable gain is most efficient when the carrier dynamics is faster than the round trip time.

Our idea is based on well established techniques for quantum dot and conventional semiconductor lasers [22–27], where PML is routinely achieved based on a saturable absorber (SA) and a gain medium as separate components of a multi-section wave guide. Here absorption is implemented by reverse biasing the gain medium. Carrying this concept to QCLs was first suggested by Kärtner [15], whereas Talukder and Menyuk were the first to point out that rather than reverse biasing the gain medium, carefully chosen positive biases should be used for QCLs [28]. In this work the authors simulated PML for MIR devices, where the intensity dependent saturation was implemented via a (slow) quantum coherent absorber. Along these lines simulations for PML in THz QCLs have also been presented [29, 30]. Here, we expand upon the previous work by (i) using an extended theoretical model, (ii) showing that guided by classical principles of mode locking [31], one can achieve PML by simply using a FSA instead, and (iii) in addition to the conventional PML approach, we also discuss the possibility of hybrid and colliding pulse mode locking (CPML).

It is interesting to note that besides quantum well structures, in principle also novel materials such as carbon nanotubes (CNTs), graphene and topological insulators can be considered to generate fast saturable absorption. Their nonlinear response is broadband and strong and can even exceed the one in intersubband quantum well structures in the THz and MIR range [32–37]. Carbon nanotube-based SAs have already been used in the near-infrared regime to achieve PML in solid state and fiber lasers [37, 38].

The way in which the FSA enables mode locking is two-fold [39, 40]. First, the FSA provides more gain for shorter pulses, strong enough to bleach the material, while at the same time it also suppresses weak background

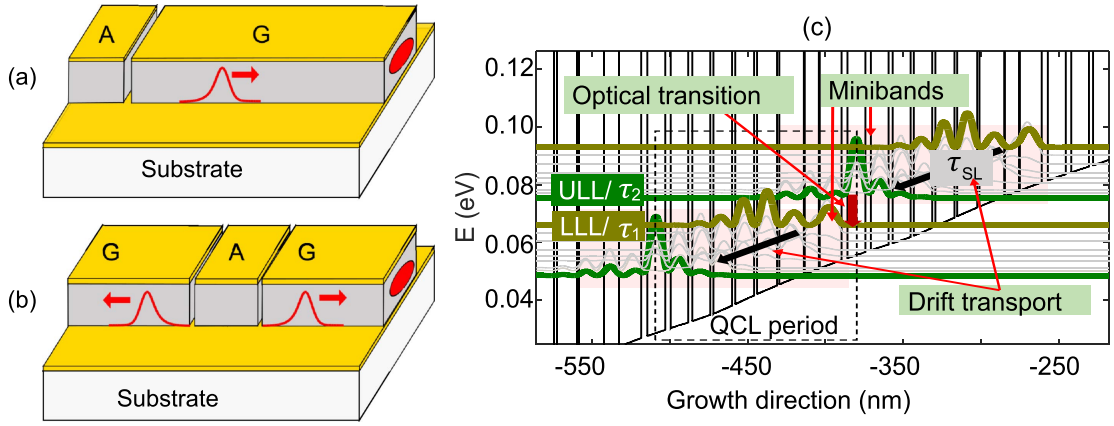

Figure 1. An example of a multi-section Fabry–Perot (FP) cavity geometry, consisting of spatially separated gain (G) and absorber (A) regions for (a) conventional passive mode locking and (b) colliding pulse mode locking. (c) Conduction band diagram and wave functions of a typical bound to continuum (BTC) GaAs/$Al_{0.15}GaAs_{0.85}$ THz quantum cascade laser (the structure is analogous to that in [41]). The upper and lower laser levels, upper laser level and lower laser level, are outlined with thick lines. The electron transport in the device is characterized by drift transport (scattering) inside the miniband and optical transitions between minibands.

fluctuations. Secondly, it also acts as a compensator for the dispersion introduced by the gain medium, as both gain and loss interact resonantly with the intracavity intensity, albeit with different signs in the polarization term. As a result, if the gain and absorber sections are packed into a compact structure, with the small round trip time only several times longer than the relaxation time in the gain section, very stable mode locking with one or two pulses per round trip arises.

This paper is organized as follows: in section 2 we present the theoretical model and in section 3 we investigate several different approaches which might lead to the generation of picosecond THz pulses via QCLs, namely conventional PML, section 3.1, CPML, section 3.2, and hybrid mode locking (HML), section 3.3.

2. Theoretical model

The multi-section cavity design envisaged by us is illustrated in figure 1 for a Fabry–Perot (FP) geometry and two different configurations, the A-G and G-A-G alignments, favoring conventional and CPML, respectively. The general geometry consists of two or more sections with different biases and effective dipole moments. Experimentally, this can be realized either via wafer-bonding of separately designed and grown structures, or by designing a single heterostructure operating either as a gain or absorber medium, depending on the driving current [42]. Additionally, a composite design employing quantum well heterostructures for the gain and CNTs, graphene or topological insulators for the SA could also be an interesting alternative [34, 35, 37]. Despite the more challenging fabrication as compared to having epitaxially stacked gain and absorption layers, or external cavity multi-section QCLs [43], we insist on monolithic waveguides as they offer two obvious advantages: (i) these structures provide short round trip lengths, and also (ii) arranging the gain and absorber in series, as depicted in the figure, allows for independent control of the injection current in all sections. Additionally, both the gain and the loss structures need to be adequately designed to satisfy the prerequisites for successful PML, and namely some $\approx$10 ps gain recovery time and fast $\approx$1 ps recovering SA, with the latter coupling more strongly to the optical field than the former.

Before we write down the equations of motion, a careful consideration of the transport processes in a BTC quantum cascade laser is in order. An example of such an active region is illustrated in figure 1(c). Typically, electron transport through the heterostructure can be described by three different lifetimes, the superlattice relaxation time, i.e. τ_{SL}, defined as the transit time of a carrier from the top of the miniband to the upper laser level, τ_2 defined as the lifetime of the upper laser level and lastly τ_1 denoting the same for the lower laser level [44].

A usual modeling approach in literature is to eliminate the population of the lower laser level, ρ_{11}, from the system of equations by assuming that $\rho_{11} \approx 0$ at all times [28, 45, 46]. This choice can be justified by the relatively fast out-scattering from this level to lower energetic states in the miniband, compared to the other non-radiative lifetimes in the system, i.e. $\tau_1 \ll \tau_2, \tau_{SL}$. Such an approximation is valid for determining the steady state solutions of the rate equations in the absence of an optical field, however it breaks down when one additionally considers photon assisted scattering, since it dramatically reduces the upper laser level lifetime [44]. Concretely, when $1/\tau_1 < 1/\tau_2 + 1/\tau_{st}(|E|^2)$, where $\tau_{st}(|E|^2)$ is the stimulated emission/absorption lifetime and

E is the electric field, the dynamics of the lower laser level can no longer be excluded, since the QCL essentially operates as a three level system [44]. A value of $\tau_1 \approx 2$ ps was reported for the first THz BTC-QCL [47], indicating that typical values for the lower laser level lifetime are of that order.

Keeping this in mind, we employ a density matrix model to describe the electron transport through the triplet $\rho_{\rm SL}$, ρ_{22} and ρ_{11} for the population density of the electrons in the miniband, the upper laser level and the lower laser level, respectively. Where necessary, we denote the various system parameters with sub-/superscript index g to indicate that those quantities are related to the gain section alone. A similar system was used in the work of Choi *et al* to provide evidence for quantum coherent dynamics in MIR QCLs, where an excellent agreement between simulation and experimental data was achieved [48].

Expanding on the usual two level Bloch equations approach, we write down the Maxwell–Bloch (MB) equations for the three level system, in the rotating wave and slowly varying amplitude approximations, taking into account counter-propagating waves and spatial hole burning. The full system of equations for the gain medium is given by

$$\frac{\partial E_{\pm}^{g}}{\partial x} \pm \frac{n_0}{c}\frac{\partial E_{\pm}^{g}}{\partial t} = -\mathrm{i}\frac{\Gamma_g \mu_g \omega_0}{\varepsilon_0 c n_0} N_g \eta_{\pm} - \frac{a}{2} E_{\pm}^{g}, \tag{1a}$$

$$\frac{\mathrm{d}\rho_{\rm SL}^{0}}{\mathrm{d}t} = \frac{\rho_{11}^{0}}{\tau_1} - \frac{\rho_{\rm SL}^{0}}{\tau_{\rm SL}}, \tag{1b}$$

$$\frac{\mathrm{d}\rho_{22}^{0}}{\mathrm{d}t} = \frac{\rho_{\rm SL}^{0}}{\tau_{\rm SL}} - \frac{\rho_{22}^{0}}{\tau_2} + \mathrm{i}\frac{\mu_g}{2\hbar}[(E_{+}^{g})^{*}\eta_{+} + (E_{-}^{g})^{*}\eta_{-} - \text{c.c.}], \tag{1c}$$

$$\frac{\mathrm{d}\rho_{11}^{0}}{\mathrm{d}t} = \frac{\rho_{22}^{0}}{\tau_2} - \frac{\rho_{11}^{0}}{\tau_1} - \mathrm{i}\frac{\mu_g}{2\hbar}[(E_{+}^{g})^{*}\eta_{+} + (E_{-}^{g})^{*}\eta_{-} - \text{c.c.}], \tag{1d}$$

$$\frac{\mathrm{d}\rho_{\rm SL}^{+}}{\mathrm{d}t} = \frac{\rho_{11}^{+}}{\tau_1} - \frac{\rho_{\rm SL}^{+}}{\tau_{\rm SL}}, \tag{1e}$$

$$\frac{\mathrm{d}\rho_{22}^{+}}{\mathrm{d}t} = \frac{\rho_{\rm SL}^{+}}{\tau_{\rm SL}} - \frac{\rho_{22}^{+}}{\tau_2} + \mathrm{i}\frac{\mu_g}{2\hbar}[(E_{-}^{g})^{*}\eta_{+} - (E_{+}^{g})\eta_{-}^{*}], \tag{1f}$$

$$\frac{\mathrm{d}\rho_{11}^{+}}{\mathrm{d}t} = \frac{\rho_{22}^{+}}{\tau_2} - \frac{\rho_{11}^{+}}{\tau_1} - \mathrm{i}\frac{\mu_g}{2\hbar}[(E_{-}^{g})^{*}\eta_{+} - (E_{+}^{g})\eta_{-}^{*}], \tag{1g}$$

$$\frac{\mathrm{d}\eta_{\pm}}{\mathrm{d}t} = -\mathrm{i}(\omega_g - \omega_0)\eta_{\pm} + \mathrm{i}\frac{\mu_g}{2\hbar}[E_{\pm}^{g}(\rho_{22}^{0} - \rho_{11}^{0}) + E_{\mp}^{g}(\rho_{22}^{\pm} - \rho_{11}^{\pm})] - \frac{\eta_{\pm}}{T_{2g}}. \tag{1h}$$

The symbols $E_{\pm}^{g}$ denote the forward and backward propagating field envelopes and $\eta_{\pm}$ the corresponding slowly varying coherence terms between the levels 1 and 2. The interference pattern of the counter-propagating waves leads to the formation of standing waves inside the cavity, which results in a population grating and consequently in spatial hole burning. According to the standard approach [18, 45, 49], we take the following ansatz for the population of the jth state

$$\rho_{jj} = \rho_{jj}^{0} + \rho_{jj}^{+}\mathrm{e}^{2\mathrm{i}k_0 x} + (\rho_{jj}^{+})^{*}\mathrm{e}^{-2\mathrm{i}k_0 x}, \tag{2}$$

where ρ_{jj}^{0} is the average population, ρ_{jj}^{+} denotes the (complex) amplitude of the grating, $k_0 = \omega_0 n_0/c$ is the carrier wave number expressed in terms of the carrier angular frequency ω_0 and the background refractive index is $n_0 \approx 3.6$. Furthermore, c denotes the velocity of light in vacuum, ε_0 the permittivity of free space and $\hbar$ the Plank constant. The rest of the simulation parameters for both absorber and gain sections are specified in table 1.

In order to impose a minimal set of assumptions about the absorber, we model it as a two level density matrix system in the rotating wave and slowly varying amplitude approximation with average inversion Δ^0, inversion grating amplitude Δ^+ and a coherence term $\pi_{\pm}$. Again, we use sub-/superscript a to specify where a particular parameter or variable relates solely to the SA. The usual MB equations read

$$\frac{\partial E_{\pm}^{a}}{\partial x} \pm \frac{n_0}{c}\frac{\partial E_{\pm}^{a}}{\partial t} = -\mathrm{i}\frac{\Gamma_a \mu_a \omega_0}{\varepsilon_0 c n_0} N_a \pi_{\pm} - \frac{a}{2} E_{\pm}^{a}, \tag{3a}$$

$$\frac{\mathrm{d}\Delta^{0}}{\mathrm{d}t} = \mathrm{i}\frac{\mu_a}{\hbar}[(E_{+}^{a})^{*}\pi_{+} + (E_{-}^{a})^{*}\pi_{-} - \text{c.c.}] - \frac{\Delta^{0} - \Delta^{\rm eq}}{T_{1a}}, \tag{3b}$$

$$\frac{\mathrm{d}\Delta^{+}}{\mathrm{d}t} = \mathrm{i}\frac{\mu_a}{2\hbar}[(E_{-}^{a})^{*}\pi_{+} - (E_{+}^{a})\pi_{-}^{*}] - \frac{\Delta^{+}}{T_{1a}}, \tag{3c}$$

$$\frac{\mathrm{d}\pi_{\pm}}{\mathrm{d}t} = -\mathrm{i}(\omega_a - \omega_0)\pi_{\pm} + \mathrm{i}\frac{\mu_a}{2\hbar}[E_{\pm}^{a}\Delta^{0} + E_{\mp}^{a}\Delta^{\pm}] - \frac{\pi_{\pm}}{T_{2a}}. \tag{3d}$$

Table 1. The parameters for the absorber (A) and gain (G) sections of the two-section ring QCL from figure 1(a). In the table below $e \approx 1.602 \times 10^{-19}$ C denotes the elementary charge.

Parameter	Unit	Value (G)	Value (A)
Dipole matrix el. (μ_j)	nm e	2	6
Resonant angular freq. (ω_j)	ps^{-1}	$3.4 \times 2\pi$	$3.4 \times 2\pi$
Gain superlattice transport time (τ_{SL})	ps	40	×
Gain upper laser level lifetime (τ_2)	ps	40	×
Gain lower laser level lifetime (τ_1)	ps	2	×
Absorber lifetime (T_{1a})	ps	×	3
Dephasing time ($T_{2a/g}$)	fs	200	160
Length (L_j)	mm	1	0.125
Doping density (N_j)	cm^{-3}	5×10^{15}	1×10^{15}
Overlap factor (Γ_j)	Dimensionless	1.0	1.0
Linear power loss (a)	cm^{-1}	10	10

By far the most well established method for the numerical analysis of mode locking in semiconductor lasers is the traveling wave model [39, 40, 50], which treats the optical field in a similar manner as in equations (1*a*) and (3*a*), however restricts the modeling of the gain/absorber dynamics to classical rate equations. This essentially 'flat gain' approximation necessitates the use of additional numerical techniques to impose the bandwidth limit of the gain medium [40]. By contrast, the MB equations intrinsically capture the spectral dependence of the gain, namely via the inclusion of the polarization equations, i.e. equations (1*h*) and (3*d*), and thus constitute a more complete model.

3. Mode locking of QCLs

In the following sections we investigate various schemes which might enable the generation of ultrashort pulses with THz QCLs. Besides conventional PML, we also treat colliding pulse and HML as alternative approaches to improve the pulse characteristics. Importantly, for our envisaged design to work, a slowly saturable gain, with inversion recovery time only several times faster than the round trip time, must be coupled to a fast saturable absorber [40]. To model this scenario we assume a parameter set as presented in table 1, with values we believe realistic for THz QCLs. Specifically, for the BTC-QCL lifetimes assumed in table 1, simulations similar to [51] yield a gain inversion lifetime of $T_{1g} \approx 12$ ps, while for the 1.125 mm FP cavity the round trip time is about 28 ps. In all of the following sections, we present results from simulations of free running, self-starting devices. To solve equations (1) and (3), we use the numerical method outlined in [13] and start all simulations from random noise. Due to the nature of the employed approximations, our results are limited to pulses with durations not significantly shorter than ~1 ps. For sub-picosecond dynamics, memory effects become also relevant, and can be taken into account by using a non-Markovian approach, however at the cost of considerably increased numerical complexity [52, 53].

3.1. Passive mode locking (PML)

One of the main results from the classical theory of PML is the condition that the absorber should saturate faster than the gain [31]. The nonlinear saturation parameter is given by $\epsilon_j = \mu_j^2 T_{1j} T_{2j} / \hbar^2$ and denotes the inverse of the saturation value of the electric field squared $|E|^2$ in each active region ($j = \{a, g\}$). When the condition $r = \epsilon_a / \epsilon_g > 1$ is met, the propagating pulse will bleach the absorber more strongly than the amplifier and thus will open a net round trip gain window. In fact, simulations for quantum dot lasers have shown [40] that the pulse duration decreases approximately exponentially with increasing value of r. Conversely, classical theory and also our simulations (results not shown here) predict that no mode locking is possible when $r < 1$ [31, 40].

Another requirement for successful mode locking is that the absorber should have a fast recovering population inversion. One can easily see the benefits of short T_{1a} lifetime for mode locking. Upon entering the absorber, the pulse front will saturate the active medium, which on the other hand will be quick enough to recover prior to arrival of the pulse tail. This type of dynamics would naturally shorten the pulse as the duration of the net gain window will decrease with decreasing T_{1a}. Following this logic, one might expect to obtain shorter pulses with decreasing absorber lifetimes, which is indeed confirmed by our simulations. Importantly, absorbers with fast carrier recovery ought to be easy to realize based on resonant phonon QCL designs, taking advantage of strong longitudinal optical phonon scattering.

Similarly to their zero-dimensional counterparts (quantum dot lasers), we argue that QCLs could be passively mode locked provided systems with suitably chosen parameters are designed. To illustrate this possibility we simulated equations (1) and (3) with a parameter set characteristic for QCLs (see table 1).

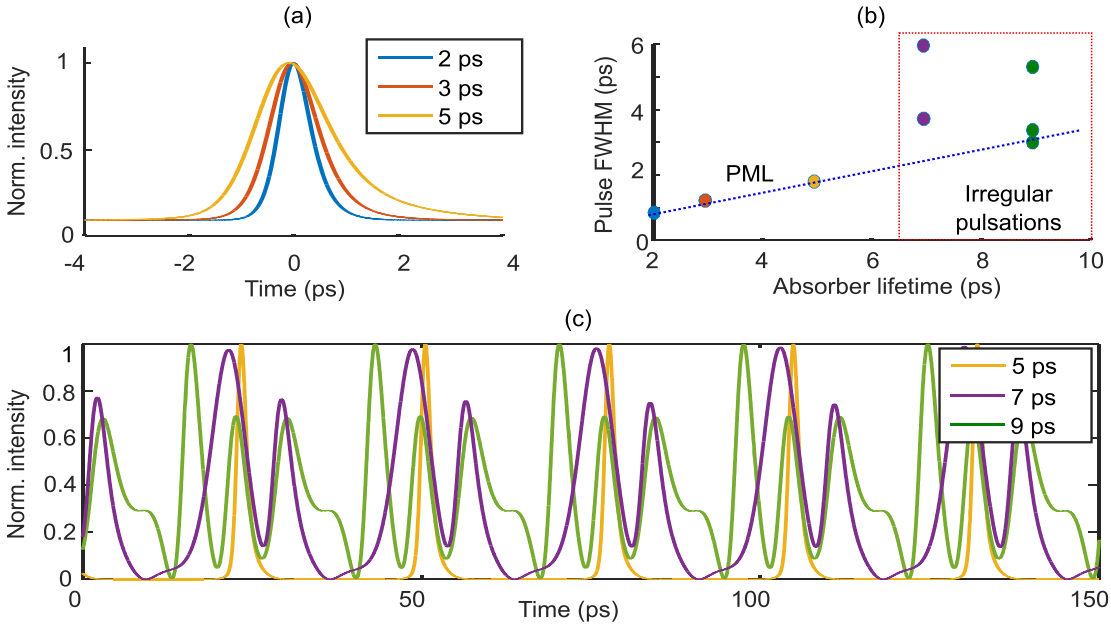

Figure 2. (a) Normalized pulse intensity versus time for values of the absorber lifetime of 2, 3 and 5 ps. (b) The intensity FWHM duration as T_{1a} is varied between 2 and 9 ps. For $T_{1a} = 7$ and 9 ps the FWHM values of the main and also the satellite pulses are presented. (c) The normalized optical intensity for $T_{1a} = 5$, 7 and 9 ps.

To investigate the importance of absorber lifetime for PML of QCLs, we varied the recovery time of the absorber between 2 and 9 ps and simulated the coupled system for around 400 round trips. Since the change of T_{1a} also changes the value of r, for each simulation we re-adjusted the absorber dipole moment in order to maintain constant r. This was necessary since we wanted to have controlled numerical experiments where only T_{1a} and not r was varied. Finally, the gain carrier density was also adjusted from its value in table 1, in order to ensure that in all subsequent simulations the active medium was biased at 1.2 times above threshold.

The results from these simulations are presented in figures 2(a) and (b) and display behavior in agreement with our expectation. When the absorber lifetime is sufficiently short the pulse duration increases with T_{2a} as seen in figure 2(a). In fact, for the PML regime in figure 2(b) we observe a clear linear relationship between T_{1a} and the intensity full width at half maximum (FWHM) pulse duration. On the other hand, for slower absorbers, the complicated interplay between the optical field and the active region dynamics produces irregular pulsations (IP) with no well defined temporal profile. From figure 2(c) we see that the onset of this regime occurs already for absorber lifetimes $T_{1a} \geqslant 7$ ps and is characterized by multiple pulses with varying intensity. Additionally, for those cases one can also observe modulation of the pulse amplitude with a period spanning several tens of round trips, a phenomenon baring resemblance to Q-switched mode locking [54]. These results unequivocally validate the important role of the absorber lifetime for the pulsation dynamics and confirm that for successful mode locking of QCLs, besides slowly saturable gain media, also absorbers with short T_{1a} lifetime and large $r = \epsilon_a/\epsilon_g$ ratio are essential.

3.2. Colliding pulse mode locking (CPML)

A special type of PML, useful for shortening even further the pulse duration, but probably more importantly to achieve high repetition rates, is the so called colliding pulse mode locking (CPML), where two gain sections of equal length are symmetrically placed around the absorber [39, 55]. When such a geometric arrangement is achieved, two identical pulses per round trip can be emitted from the device, resulting in doubled repetition rate equal to the second harmonic of the round trip frequency. In fact, we expect that CPML will be easier to achieve via BTC quantum cascade lasers as the short gain recovery time will naturally favor such multi-pulse regime of operation [29].

To understand why CPML occurs, consider the schematic in figure 1(b), illustrating a multi-section cavity design in the G-A-G (gain-absorber-gain) configuration. Let us assume that a single pulse with amplitude E_0 propagates inside a gain medium with some group velocity v_g. Close to the resonator mirrors, during its forward pass the pulse will saturate the gain and there will be not enough time for the latter to recover in order to re-amplify the reflected signal. This leads to a reduction of the effective length of the gain medium by $\Delta L = v_g \tau_{gr}/2$, which is half the distance traveled by the pulse in time τ_{gr}, where $\tau_{gr} \neq T_{1g}$ denotes the time it takes for the gain to recover to its threshold value. In a two level system approximation, it can be shown that τ_{gr} is a monotonously increasing function of $|E_0|^2$, and as such ΔL will be shorter if the pulse would split into two

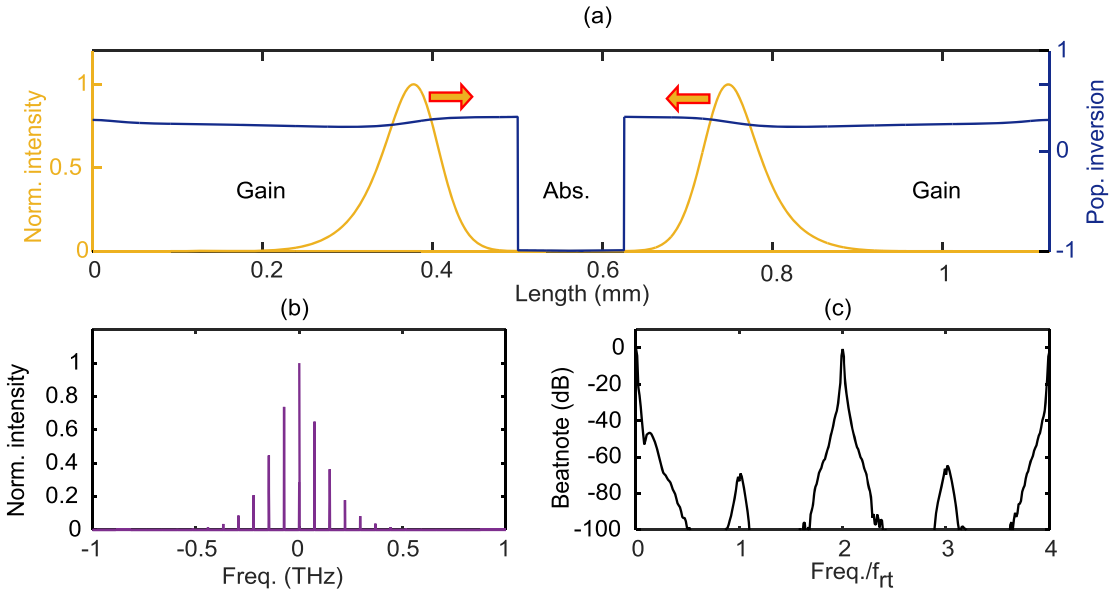

Figure 3. (a) A snapshot of the optical intensity (left y-axis) and population inversion (right y-axis) inside the cavity. (b) Optical spectrum of the field emitted from the right facet of the cavity. (c) A log plot of the beatnote signal versus frequency (normalized to the cavity round trip frequency $f_{\rm rt}$) produced by the device.

identical copies with *half* the total intensity each, since then $\tau_{\rm gr}$ will also decrease. The most stable two-pulse configuration in a G-A-G FP cavity are indeed pulses, colliding in the cavity center, as those will saturate the absorber more deeply and further reduce the round trip losses.

To confirm these expectations, we simulated equations (1) and (3) in the G-A-G arrangement for the parameter set in table 1. Figure 3 illustrates the results. After about 50 round trips the laser emission transforms into two identical counter-propagating pulses which collide inside the center of the cavity, figure 3(a). The spectrum in figure 3(b) consists of more than 15 modes separated by twice the round trip frequency, $f_{\rm rt}$, whereas beatnote calculations, figure 3(c), indicate a strong component at the second harmonic of $f_{\rm rt}$. We simulated over hundreds of round trips to confirm the stability of the second harmonic regime, and the given beatnote linewidths in figure 3(c) are limited by the Fourier transform resolution of our simulations. Such a device essentially represents a very stable local oscillator with a repetition frequency of around ≈71 GHz [56].

3.3. Hybrid mode locking (HML)

As shown above, the multi-section gain/SA system might lase in a regime of irregular pulsations [39]. In order to enforce phase-locking of the modes, one can additionally modulate the current/voltage of the gain or the absorber at the round trip frequency of the optical field. Such a hybrid approach could be envisaged for QCLs, where the applied bias of the absorber is superimposed with a sinusoidally varying radio frequency (RF) source via a bias-T, and the gain medium is pumped with a DC current (see figure 4(a)) [26, 57].

In fact, HML is a well established technique, which is commonly used for pulse repetition frequency stabilization in passively mode locked semiconductor lasers. Fundamentally, HML is a combination of PML and active mode locking, where most often the external RF voltage modulation is applied to the SA section. As such, if the modulation frequency is close to the cavity repetition frequency, the PML repetition rate can lock to the frequency of the external voltage. This interval, where the locking takes place, is referred to as the locking range, and the overall mechanism of fixing the cavity round trip frequency to an external local oscillator is termed as injection locking. For terahertz QCLs, this frequency stabilization technique was already studied in detail, where, for example, it was shown that metal–metal waveguides are more suitable than surface-plasmon such for that particular purpose [58]. For a more detailed theoretical description of HML of semiconductor lasers, we refer the reader to [26].

To simulate this technique we introduced the term $m_0 \sin(2\pi f_{\rm rt} t)$ in the right hand side of equation (3*b*), modeling the RF source [49], where the modulation amplitude was set to 25% of the DC current, i.e. $m_0 = 0.25 \times \Delta_a^{\rm eq}/T_{1a}$. Again, we repeated the simulations from figure 2 to evaluate how effective this active +passive mode locking will be as compared to the simple PML case. The results are plotted in figure 4(b).

From figure 4(b), within the fast absorber regime (i.e. $T_{1a} = 2$–5 ps), we see that applied RF modulation does not seem to have any significant impact on the pulse widths, as the calculated FWHM-values are of almost the same magnitude as in figure 2(b). This is not so surprising as the laser already operates in a mode locking regime

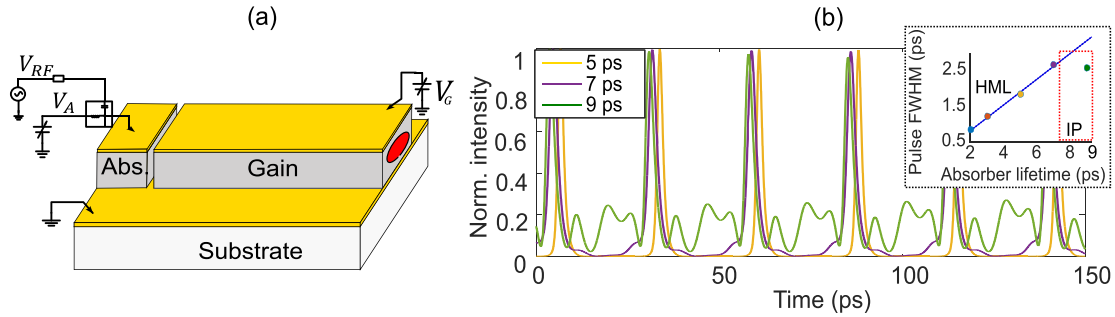

Figure 4. (a) Schematic diagram of hybrid mode locking with RF modulation of the absorber bias. (b) Intensity profile for $T_{1a} = 5, 7$ and 9 ps. (Inset) Intensity FWHM versus absorber lifetime for the hybrid configuration of (a) and the same parameter set as the one which produced the results in figure 2(b).

and so additional RF-injection would have little to no effect on the dynamics. However, substantial improvement in the pulse structure and duration is observed for slower absorbers as the satellite pulsations are strongly suppressed in favor of more regular pulses. In particular, comparing the time-domain profile of the intensity in figures 2(c) and 4(b), we see that as a result of this additional active modulation the pulse at $T_{1a} = 7$ ps has completely recovered its integrity whereas the pulse substructures for $T_{1a} = 9$ ps are drastically reduced. Again, drawing insights from the semiconductor laser community [59, 60], one might expect that with this HML technique an improvement in the overall stability of the pulse train and mode locking parameter range can be achieved, as compared to the passive mechanism alone.

4. Conclusion

We have suggested feasible approaches for ultrashort pulse generation in self-starting BTC terahertz quantum cascade lasers. Our scheme is based on the realization of a paradigmatic model for passive mode locking via a fast saturable absorber, implementable via multi-section monolithic FP cavities. We predict the formation of short picosecond pulses with FWHM limited by the gain bandwidth of the device. Our investigations show that besides a suitably engineered gain medium with slowly recovering population inversion, a fast absorber with very strong coupling to the optical field is essential. Carefully conducted numerical experiments indicate that the multi-section configuration is prone to entering into a regime of irregular pulsations if the absorber recovery time is very large, which should be an important point to consider in future designs. Furthermore, besides PML, we have also discussed alternative approaches to ultrashort pulse generation in QCLs, i.e. hybrid and colliding pulse mode locking. By utilizing active modulation of the injection current in the absorber, the former method recovers the regular pulsations from an irregular regime. On the other hand, CPML might be easier to achieve with THz QCLs as multi-pulse lasing is the naturally preferred mode of operation in fast gain recovery active media.

Funding Information

This work was supported by the German Research Foundation (DFG) within the Heisenberg program (JI 115/4-2) and under DFG Grant No. JI 115/9-1 and the Technical University of Munich (TUM) in the framework of the Open Access Publishing Program. IB and UM are thankful for the financial support by DFG grants BA 4156/4-1 and MO 850-19/1. NR thanks Russian Foundation for Basic Research, project no. 16-02-00762a.

ORCID iDs

I Babushkin https://orcid.org/0000-0001-9686-0811
R Arkhipov https://orcid.org/0000-0002-3109-8237
C Jirauschek https://orcid.org/0000-0003-0785-5530

References

[1] Williams B S 2007 *Nat. Photon.* **1** 517
[2] Faist J, Capasso F, Sivco D L, Sirtori C, Hutchinson A L and Cho A Y 1994 *Science* **264** 553
[3] Bai Y, Darvish S, Slivken S, Zhang W, Evans A, Nguyen J and Razeghi M 2008 *Appl. Phys. Lett.* **92** 101105

[4] Fathololoumi S, Dupont E, Chan C, Wasilewski Z, Laframboise S, Ban D, Mátyás A, Jirauschek C, Hu Q and Liu H 2012 *Opt. Express* **20** 3866
[5] Hugi A, Villares G, Blaser S, Liu H and Faist J 2012 *Nature* **492** 229
[6] Burghoff D, Kao T Y, Han N, Chan C W I, Cai X, Yang Y, Hayton D J, Gao J R, Reno J L and Hu Q 2014 *Nat. Photon.* **8** 462
[7] Ulbricht R, Hendry E, Shan J, Heinz T F and Bonn M 2011 *Rev. Mod. Phys.* **83** 543
[8] Wang F *et al* 2015 *Optica* **2** 944
[9] Barbieri S, Ravaro M, Gellie P, Santarelli G, Manquest C, Sirtori C, Khanna S P, Linfield E H and Davies A G 2011 *Nat. Photon.* **5** 306
[10] Bachmann D, Rösch M, Süess M J, Beck M, Unterrainer K, Darmo J, Faist J and Scalari G 2016 *Optica* **3** 1087
[11] Paiella R, Capasso F, Gmachl C, Sivco D L, Baillargeon J N, Hutchinson A L, Cho A Y and Liu H 2000 *Science* **290** 1739
[12] Wang C Y *et al* 2009 *Opt. Express* **17** 12929
[13] Tzenov P, Burghoff D, Hu Q and Jirauschek C 2016 *Opt. Express* **24** 23232
[14] Haus H A 2000 *IEEE J. Sel. Top. Quantum Electron.* **6** 1173
[15] Kärtner F 2008 Instabilities and mode locking of quantum cascade lasers *IQCLSW 2008 Conf. (Ascona, Switzerland, 14–19 September 2008)* (https://iqclsw.phys.ethz.ch/pres/kaertner16.pdf)
[16] Kärtner F, Aus Der Au J and Keller U 1998 *IEEE J. Sel. Top. Quantum Electron.* **4** 159
[17] Jirauschek C 2017 *J. Appl. Phys.* **122** 133105
[18] Wang C Y *et al* 2007 *Phys. Rev.* A **75** 031802
[19] Jirauschek C and Lugli P 2009 *J. Appl. Phys.* **105** 123102
[20] Green R P, Tredicucci A, Vinh N Q, Murdin B, Pidgeon C, Beere H E and Ritchie D A 2009 *Phys. Rev.* B **80** 075303
[21] Bacon D R, Freeman J R, Mohandas R A, Li L, Linfield E H, Davies A G and Dean P 2016 *Appl. Phys. Lett.* **108** 081104
[22] Avrutin E, Marsh J and Portnoi E 2000 *IEE Proc.—Optoelectron.* **147** 251
[23] Vladimirov A G and Turaev D 2005 *Phys. Rev.* A **72** 033808
[24] Rafailov E, Cataluna M, Sibbett W, Ilinskaya N, Zadiranov Y M, Zhukov A, Ustinov V, Livshits D, Kovsh A and Ledentsov N 2005 *Appl. Phys. Lett.* **87** 081107
[25] Rafailov E, Cataluna M and Sibbett W 2007 *Nat. Photon.* **1** 395
[26] Arkhipov R, Pimenov A, Radziunas M, Rachinskii D, Vladimirov A G, Arsenijević D, Schmeckebier H and Bimberg D 2013 *IEEE J. Sel. Top. Quantum Electron.* **19** 1100208
[27] Arkhipov R, Arkhipov M, Babushkin I and Rosanov N 2016 *Opt. Lett.* **41** 737
[28] Talukder M A and Menyuk C R 2014 *Opt. Express* **22** 15608
[29] Tzenov P, Arkhipov R, Babushkin I, Sayadi O, Rosanov N, Morgner U and Jirauschek C 2017 *Lasers and Electro-Optics Europe & European Quantum Electronics Conf. (2017 Conf. on CLEO/Europe-EQEC)* (Piscataway, NJ: IEEE) p 1
[30] Talukder M A 2017 *Image Sensing Technologies: Materials, Devices, Systems, and Applications IV* vol 10209 (International Society for Optics and Photonics) p 1020906
[31] Haus H A 1975 *J. Appl. Phys.* **46** 3049
[32] Yao X, Tokman M and Belyanin A 2014 *Phys. Rev. Lett.* **112** 055501
[33] Hartmann R R, Kono J and Portnoi M E 2014 *Nanotechnology* **25** 322001
[34] Zheng Z, Zhao C, Lu S, Chen Y, Li Y, Zhang H and Wen S 2012 *Opt. Express* **20** 23201
[35] Chen S, Zhao C, Li Y, Huang H, Lu S, Zhang H and Wen S 2014 *Opt. Mater. Express* **4** 587
[36] Chen Y C, Raravikar N, Schadler L, Ajayan P, Zhao Y P, Lu T M, Wang G C and Zhang X C 2002 *Appl. Phys. Lett.* **81** 975
[37] Schmidt A *et al* 2008 *Opt. Lett.* **33** 729
[38] Set S Y, Yaguchi H, Tanaka Y and Jablonski M 2004 *J. Lightwave Technol.* **22** 51
[39] Jones D, Zhang L, Carroll J and Marcenac D 1995 *IEEE J. Quantum Electron.* **31** 1051
[40] Williams K, Thompson M and White I 2004 *New J. Phys.* **6** 179
[41] Barbieri S, Alton J, Beere H E, Fowler J, Linfield E H and Ritchie D A 2004 *Appl. Phys. Lett.* **85** 1674
[42] Schwarz B, Reininger P, Ristanić D, Detz H, Andrews A M, Schrenk W and Strasser G 2014 *Nat. Commun.* **5** 4085
[43] Revin D, Hemingway M, Wang Y, Cockburn J and Belyanin A 2016 *Nat. Commun.* **7** 11440
[44] Choi H, Diehl L, Wu Z K, Giovannini M, Faist J, Capasso F and Norris T B 2008 *Phys. Rev. Lett.* **100** 167401
[45] Gordon A *et al* 2008 *Phys. Rev.* A **77** 053804
[46] Jirauschek C and Kubis T 2014 *Appl. Phys. Rev.* **1** 011307
[47] Köhler R, Tredicucci A, Beltram F, Beere H E, Linfield E H, Davies A G, Ritchie D A, Iotti R C and Rossi F 2002 *Nature* **417** 156
[48] Choi H, Gkortsas V M, Diehl L, Bour D, Corzine S, Zhu J, Höfler G, Capasso F, Kärtner F X and Norris T B 2010 *Nat. Photon.* **4** 706
[49] Gkortsas V M, Wang C, Kuznetsova L, Diehl L, Gordon A, Jirauschek C, Belkin M, Belyanin A, Capasso F and Kärtner F 2010 *Opt. Express* **18** 13616
[50] Yang W and Gopinath A 1993 *Appl. Phys. Lett.* **63** 2717
[51] Talukder M A 2011 *J. Appl. Phys.* **109** 033104
[52] Butscher S, Förstner J, Waldmüller I and Knorr A 2005 *Phys. Rev.* B **72** 045314
[53] Knezevic I and Novakovic B 2013 *J. Comput. Electron.* **12** 363
[54] Brovelli L R, Kopf D and Kamp M 1995 *Opt. Eng., Bellingham* **34** 2024
[55] Chen Y K and Wu M C 1992 *IEEE J. Quantum Electron.* **28** 2176
[56] Sonnabend G, Wirtz D and Schieder R 2005 *Appl. Opt.* **44** 7170
[57] Fiol G, Arsenijević D, Bimberg D, Vladimirov A, Wolfrum M, Viktorov E and Mandel P 2010 *Appl. Phys. Lett.* **96** 011104
[58] Gellie P *et al* 2010 *Opt. Express* **18** 20799
[59] Derickson D J, Morton P, Bowers J and Thornton R 1991 *Appl. Phys. Lett.* **59** 3372
[60] Thompson M *et al* 2003 *Electron. Lett.* **39** 1121